

*Sp*  
*2mix*

MCR-73-322

CONTRACT NAS8-29013

FINAL SUMMARY REPORT

N74-21069

(NASA-CR-120130) THE FABRICATION AND  
TEST OF A DUAL SPIN GAS BEARING REACTION  
WHEEL Final Summary Report (Martin  
Marietta Corp.)

54 p HC

CSCL 131

Unclas

G3/15 16089

THE FABRICATION AND TEST OF  
A DUAL SPIN GAS BEARING  
REACTION WHEEL

November 1973

Prepared for:

GEORGE C. MARSHALL  
SPACE FLIGHT CENTER  
MARSHALL SPACE FLIGHT CENTER, ALA

MARTIN MARIETTA CORPORATION  
P. O. Box 179  
Denver, Colorado

Reproduced by  
NATIONAL TECHNICAL  
INFORMATION SERVICE  
U.S. Department of Commerce  
Springfield, VA. 22151

UNCLASSIFIED

MCR-73-322  
CONTRACT NAS8-29013

FINAL SUMMARY REPORT

---

THE FABRICATION AND TEST OF  
A DUAL SPIN GAS BEARING  
REACTION WHEEL

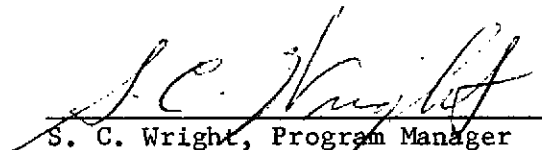
November 1973

Prepared for:

GEORGE C. MARSHALL  
SPACE FLIGHT CENTER  
MARSHALL SPACE FLIGHT CENTER, ALA

Prepared by:

R. L. Oppen and W. J. Owen  
Co-Authors

  
S. C. Wright, Program Manager  
Applications Section - 0472  
Science and Applications Department

MARTIN MARIETTA CORPORATION  
P. O. Box 179  
Denver, Colorado 80201

FOREWORD

---

This document is the final summary report submitted by Martin Marietta Corporation in accordance with Contract NAS8-29013.

PRECEDING PAGE BLANK NOT FILMED

## ABSTRACT

---

This final summary report sets forth design and fabrication activities, calculations\* and data, and conclusions associated with fabrication and test of a dual spin gas bearing reaction wheel in accordance with requirements of Contract NAS8-29013.

Under the contract, a dual spin gas bearing reaction wheel with a nominal momentum of  $\pm 6.8$  N-m-s (5 ft-lb sec) was delivered to Marshall Space Flight Center on 16 November 1973. The unique feature of this reaction wheel is the dual gas bearing concept in which two sets of self-acting hydrodynamic bearings are employed to obtain stictionless operation and low-noise around zero speed, and accommodate the momentum range from plus 6.8 N-m-s to minus 6.8 N-m-s with the potential for long life inherent in the gas bearing.

All objectives of the contract have been met and the dual spin gas bearing reaction wheel, fully functional, has been demonstrated and delivered.

There is a patent pending on the dual spin gas bearing concept. The inventor is Mr. R. L. Gates and the patent will be assigned to Martin Marietta Corporation.

-----

\* All calculations have been performed in English units and then converted to SI units.

# TABLE OF CONTENTS

	<u>Page No.</u>
List of Figures . . . . .	v
List of Tables . . . . .	vi
1.0 Summary of Accomplishments . . . . .	1
2.0 Design and Functional Description . . . . .	3
2.1 Specification . . . . .	3
2.1.1 Functional Performance . . . . .	3
2.1.2 Environmental Requirements . . . . .	3
2.2 Functional Description . . . . .	3
2.3 Calculations and Design Criteria . . . . .	4
2.4 Size and Weight . . . . .	9
2.5 Calculated Performance . . . . .	9
2.6 Motor Characteristics . . . . .	10
2.7 Materials . . . . .	13
2.8 Fabrication of Precision Bearing Parts . . . . .	13
3.0 Tests . . . . .	15
3.1 Summary of Tests after Assembly . . . . .	15
3.2 Acceptance Tests . . . . .	17
4.0 Conclusions and Recommendations . . . . .	17

## APPENDIX

- A. Acceptance Test Report and Operating Procedure
- B. List of Drawings
- C. Specification

LIST OF FIGURES

---

	<u>Page No.</u>
1.0-1 Dual Spin Gas Bearing Reaction Wheel	5
1.0-2 Bearing Components	5
2.2-1 Cross Section of Dual Spin Gas Bearing Reaction Wheel	6
2.2-2 Conventional Spherical Gas Bearing Reaction Wheel	7
2.2-3 Dual Spin Gas Bearing Reaction Wheel	7
2.5-1 Stability Map for Angular Motion of the Rotating Assembly	12
3.1-1 Block Diagram of Test Setup	16

TABLES

---

	<u>Page No.</u>
1.0-I Summary of Performance	2
2.5-I Calculated Nominal Performance	11

## 1.0 SUMMARY OF ACCOMPLISHMENTS

The accomplishments of this task have been in complete compliance with Contract NAS8-29013. A dual spin gas bearing reaction wheel with 6.8 N-m-s (5 ft-lb sec) capability has been fabricated, tested, and delivered. The dual spin gas bearing reaction wheel employs a novel concept that achieves a self-contained hydrodynamic gas spin bearing that can be stopped and reversed without bearing touchdown. The major advantages of this concept are: (1) practically unlimited wear life, and (2) the absence of stiction at zero speed. Design parameters for this bearing were previously established by Martin Marietta independent research and development activities and our subcontractors.

The piece parts for the reaction wheels were manufactured by Mechanical Technology Incorporated (MTI), Latham, New York; Speedring Systems, Warren, Michigan; Schaeffer Magnetics, Chatsworth, California; Millis Research, Millis, Massachusetts; and Teledyne Gurley, Troy, New York. The completed assembly was fabricated and tested at MTI.

The fabricated reaction wheel and its parts are shown in Figure 1.1-1.

The reaction wheel has been tested to confirm performance and demonstrate the concept. The basic parameters tested were:

- 1) bearing stiffness;
- 2) bearing stability;
- 3) power losses;
- 4) voltage versus speed characteristics.



# PERFORMANCE SUMMARY

## DUAL SPIN GAS BEARING REACTION WHEEL:

. REACTION TORQUE	-0.18 to +0.32 N-m	(25 to 45 oz-in)
. MOMENTUM STORAGE	6.8 N-m-s	(5-ft-lb-sec)
. TORQUE NOISE		0.01%
. POTENTIAL LIFE	$3.15 \times 10^8$ s	( 10 years)
. WEIGHT	13.6 Kg	( 30 lb <sup>*</sup> )
. BEARING POWER LOSS (MAX)		(20.14 watts <sup>*</sup> )
. DESIGNED FOR 0.052 rad/s ( $3^\circ$ /sec) BODY RATE		
. DESIGNED FOR NORMAL LAUNCH ENVIRONMENTS		

-----  
 \* Considerable savings potential

Table 1.0-I

## 2.0 DESIGN AND FUNCTIONAL DESCRIPTION

### 2.1 Specification

#### 2.1.1 Functional Performance

The specification for the dual spin gas bearing reaction wheel is for a bidirectional gas bearing reaction wheel that will demonstrate a strong potential for long operating life, stictionless operation around zero speed, low self-generated noise, and torque resolution limited only by motor and support electronics technology. The performance specifications follow.

Momentum: The inertial rotor momentum capability shall be in the 3 to 5 ft-lb sec range (plus and minus);

Drive Motors: Middle spin structure shall be driven by a brushless ac motor(s);

Inertial rotor motor(s) shall be either an ac or dc brushless type;

Bearing: The gas bearing shall employ spherical, spiral groove "pumps" and shall be treated to permit repeated start-stop operation.

Tachometer: Mechanization capable of measuring relative rate between the inertia rotor and the case is required.

Body-Rate Capability: The bearing design shall be such that neither touchdown nor instabilities occur when rates as high as  $\pm 3$  deg/sec exist about an axis normal to the spin axis of the momentum wheel for the momentum range.

Bearing and Windage Losses: The reaction wheel shall be designed such that the combined inner and outer bearing losses plus the windage loss shall not exceed 5 watts/ft-lb sec (maximum wheel design value) under the worst case internal pressure and temperature, operating at maximum momentum in the counter rotating mode, in a zero gravity field.

#### 2.1.2 Environmental Requirements (See Appendix C.)

### 2.2 Functional Description

A cross section of the dual spin gas bearing reaction wheel is shown in Figure 2.2-1. This figure shows a thin spun aluminum cover; however, the unit fabricated under this contract has a modified cover to facilitate testing. The wheel is the inertial element that is driven by the induction motor to achieve momentum range. The hysteresis motor drives the middle spin element at a constant speed. The optical encoder is the speed sensing device that provides a measure of wheel speed (momentum) and the change in momentum (torque). The principle of operation can be described by first comparing the concept to the conventional gas bearing.

The conventional application of a spherical gas bearing to an inertia wheel is shown in cross-section in Figure 2.2-2. When the rotor spins, spiral grooves, employed to provide both stability and stiffness, develop support

pressure allowing the bearing to run on a thin gas film with no mechanical contact. However, rotor direction cannot be reversed because the grooves are directional and support forces would be lost.

The dual spin gas bearing reaction wheel employs a middle spin structure to make the bearing bidirectional. Figure 2.2-1 illustrates the arrangement. The middle spin element rotates at constant speed in a single direction, and the wheel rotates at variable speed in either direction, and the wheel rotates at variable speed in either direction, but always slower than the middle spin element. There are two gas bearings in cascade. The inner gas bearing film is between the middle spin element and the central hemispherical stator. The outer gas bearing film is between the middle spin element and the wheel. Each rotating member is driven by its own separate motor. The middle spin motor is a hysteresis synchronous motor, and the reaction wheel motor is a two-phase servo induction motor.

The synchronous motor runs at constant speed, driving the middle spin element unidirectionally. The outer surface of the stator elements are provided with spiral grooves. Thus, the relative motion between the stator and the middle spin element pumps a gas film that supports the middle spin element. The middle spin element is also provided with spiral pumping grooves on its outer (convex surface). Therefore, it too will pump a support film between itself and the reaction wheel hub, so long as there is a sufficient relative velocity between the reaction wheel and the middle spin element. The relative velocity must, of course, be in the proper direction with respect to the spiral grooves. The condition is satisfied for this particular design by never operating the wheel at more than half the middle spin element speed. Because the two gas support films are in cascade, the inner film must support the weight of both itself and that of the reaction wheel, as well as provide adequate angular stiffness to avoid touchdown due to gyroscopic forces resulting from angular turning rates about axes not coincident with the spin axis.

### 2.3 Calculations and Design Criteria

The basic criteria in sizing the bearings were 1) both the inner and outer gas bearings must be capable of supporting the weight of the rotating assembly in a one-g field in either horizontal or vertical attitude, and both gas bearings have to support the gyroscopic torque loads corresponding to cross axis body rates up to  $\pm 0.052$  rad/s ( $\pm 3$  deg/sec). The eccentricity ratio under the maximum combination of loads has to be no greater than 0.5; 2) the combined gas bearing system must be dynamically stable with respect to axial, radial, and angular excitations over full-speed ranges.

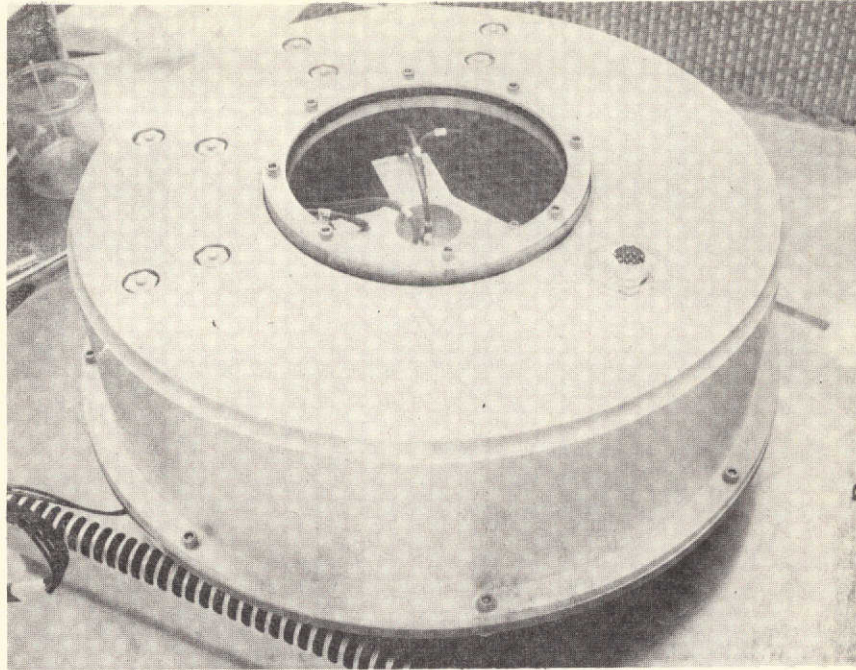


Figure 1.0-1 Dual Spin Gas Bearing Reaction Wheel

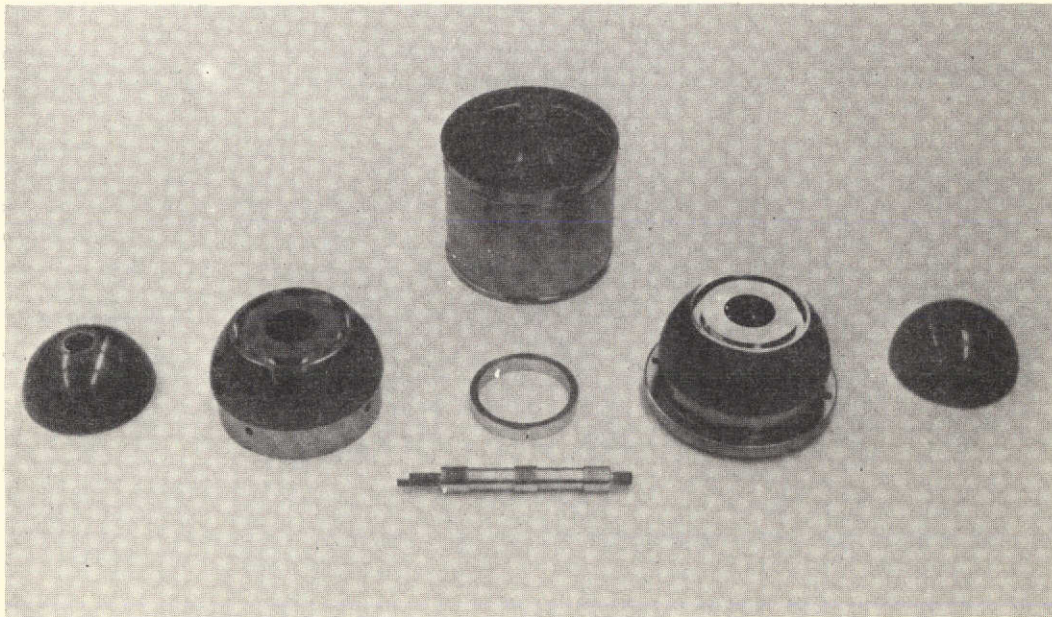


Figure 1.0-2 Bearing Components

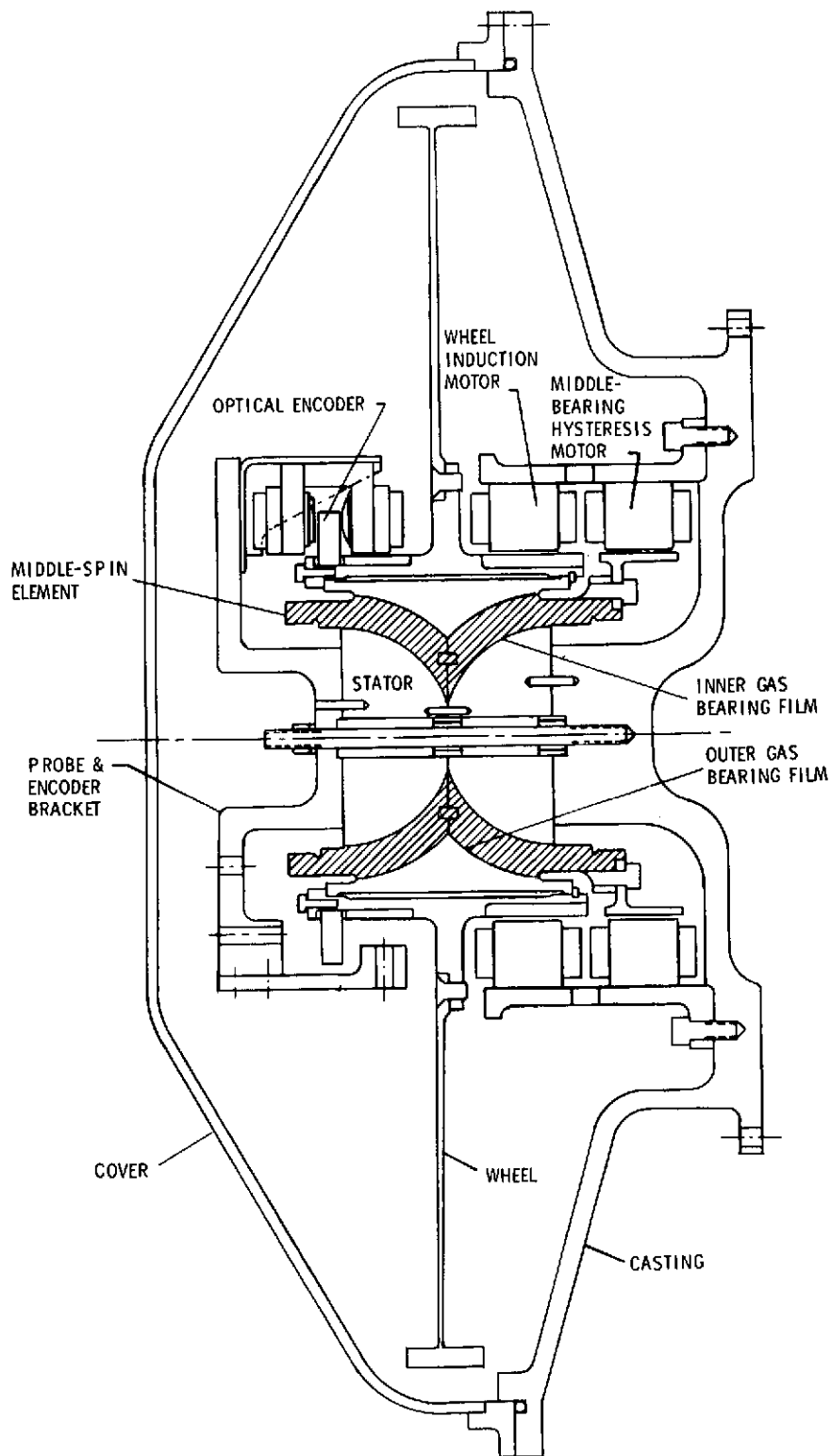


Figure 2.2-1 Cross Section of Dual Spin Gas Bearing Reaction Wheel

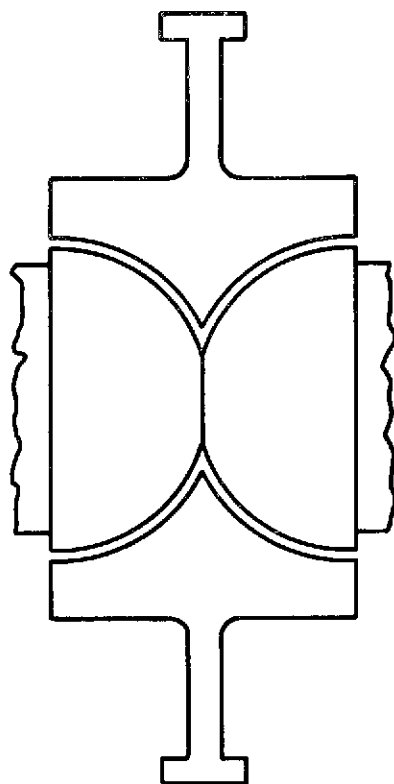


Figure 2.2-2 Conventional Spherical Gas Bearing Reaction Wheel

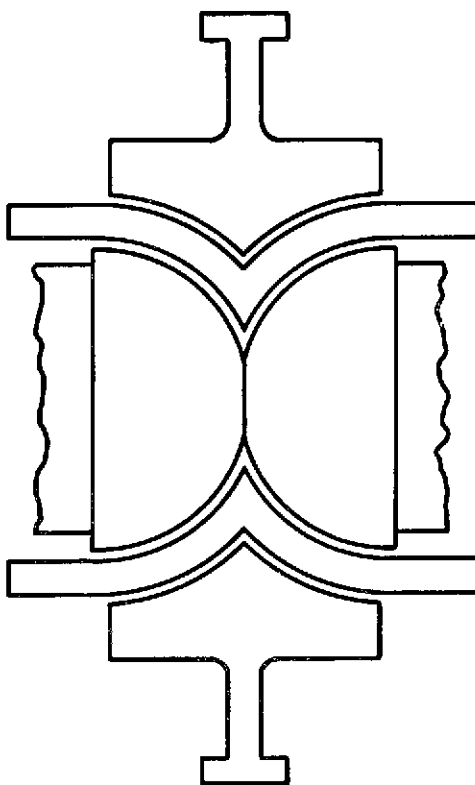


Figure 2.2-3 Dual Spin Gas Bearing Reaction Wheel

These criteria are expressed as

$$(K_a)_{i,o} > \frac{Mg}{\frac{1}{2}(h_a)_{i,o}}$$

$$(K_r)_{i,o} > \frac{Mg}{\frac{1}{2}(h_r)_{i,o}}$$

$$(K_\theta)_{i,o} > \frac{Mg}{\frac{1}{2}(\theta)_{i,o}}$$

$$M_{cr_a} > M_M + M_W$$

$$M_{cr_r} > M_M + M_W$$

$$I_{cr} > I_M + I_W$$

where the subscripts  $i$  and  $o$  apply to the inner and outer gas bearing films, respectively.  $K_a$ ,  $K_r$ , and  $K_\theta$  are axial, radial, and angular stiffnesses of the gas films;  $h_a$ ,  $h_r$ , and  $\theta$  are the axial, radial, and angular clearances of the gas bearing film, respectively. These clearances are a function of the bearing geometry.

As previously mentioned, self-acting gas bearings are also subject to self-excited instabilities, particularly when operating at or near zero eccentricity. These instability thresholds are most often defined in terms of critical mass and critical inertia. These criteria,  $M_{cr_a}$ ,  $M_{cr_r}$ , and  $I_{cr}$  are the

axial critical mass, the radial critical mass, the critical transverse inertia, respectively, associated with the combined (inner and outer) gas-bearing system. For stable operation, actual mass of the rotating assembly must be less than the smaller of  $M_{cr_a}$  and  $M_{cr_r}$ . Similarly, actual transverse inertia of

the rotating assembly must be less than  $I_{cr}$ . For the spherical nonvented configuration the system is essentially inherently stable with regard to axial excitations.

Values of stiffness of the individual bearings and critical mass and critical inertia of the combined, two-bearing system were calculated by Mechanical Technology Incorporated, using their CADENCE-42 computer program for spherical compressible flow, spiral-grooved bearings. To optimize the bearing design, MTI also used an auxiliary program that calculates the combination of bearing size, operating speed, and ambient pressure, such that all criteria expressed in the equations for the specified momentum level are satisfied with minimum power loss. The power loss is simply the sum of viscous friction losses in the inner and outer gas bearing films plus the windage loss.

The drawings set forth in the Appendix B represent the design resulting from these calculations.

#### 2.4 Size and Weight

The wheel diameter is 0.356 m (14 in.). The curve of power versus diameter for a 6.8 N-m-s (5 ft-lb sec) momentum flattens at this point and this diameter was chosen as best. The overall diameter of the housing is approximately 0.381 m (15 in.). Figure 2.1-1 shows attachment of the rotating assembly by the inner bearing member (or stator) directly to a casting which serves as one of the two pieces of the housing. The other housing part (cover) is an aluminum turning which is sealed to the casting by an O-ring. The cover serves as a panel for bringing out various instrumentation feed-throughs for test purposes. The total weight of the reaction wheel assembly is 15.97 kg.

#### 2.5 Calculated Performance

Table 2.5-I shows calculated performance over the range of wheel speeds. Each design criterion defined in the previous section is compared with the calculated performance, and a "safety factor" computed. For eccentricity ratios, this factor is defined as:

$$\text{safety factor} = \frac{\text{bearing load at an eccentricity ratio of 0.5}}{\text{actual bearing load}}$$

For system stability, the safety factor is defined as:

$$\text{safety factor} = \frac{\text{critical mass (or inertia)}}{\text{actual mass (or inertia)}}$$

Table 2.5-I shows that the gas bearing system satisfied all the design criteria. The most critical conditions occur during maximum co-rotation and when the bearing clearance is at the high end of the tolerance band. Even at this condition, there is about 20% margin of system stability. The margin increases very rapidly as wheel speed is reduced, or if the clearance is less than the maximum value. In horizontal operation in a one-g field, the safety factors on load capacity, i.e., on radial eccentricity ratios, are all very high (greater than three in all cases). In vertical operation in a one-g field, the axial load capacity of the outer bearing has a minimum margin of 40% (based on a maximum allowable eccentricity ratio of 0.5). This also occurs in maximum co-rotation, and the safety factor increases rapidly as the wheel speed is reduced.



The effect of the maximum body rate of  $\pm 0.052$  rad/s ( $\pm 3$  deg/sec) on the gas bearings is small. The moment load due to this body rate produces eccentricity ratios less than 0.1 in all cases.

The most critical operating condition will occur in zero-g, where the radial and axial eccentricity ratios will all be near zero. However, the same stability limits (critical mass and critical inertia) noted in Table 2.5-I will apply, as will eccentricity ratios due to the body rate. The region of possible operation of the gas bearing assembly is illustrated in the stability map (Figure 2.5-I). This shows that operation should be fully stable over the complete speed range of the wheel and in the range of bearing clearances.

## 2.6 Motor Characteristics

Two motors are required to operate the dual spin gas bearing. One is needed to drive the middle spin element unidirectionally at essentially constant speed, and the other to drive the outer hub or reaction wheel in either direction at varying commanded speeds.

The motor for the middle spin element is a two-phase synchronous motor. The motor specification follows.

### Hysteresis Motor

Number of Poles	- 30
Starting Torque	- 0.226 N-m (32 oz-in.) (momentary over-voltage excitation permissible);
Load Torque Capability	- 0.090 N-m (12.7 oz-in.) minimum without pulling out of synchronism;
Excitation	- two-phase 800 Hz, 35V rms sinewave both phases.

The synchronous motor has a frameless pancake configuration; the design is conventional except for its high pole density. The speed requirement is 336 rad/s (3200 rpm) at 800 Hz.

The reaction wheel motor is a two-phase servo frameless pancake induction motor that permits reasonably linear open-loop speed control in either direction. It is a 30-pole motor and runs at only 167.5 rad/s (1600 rpm) maximum, and requires about one-half of rated excitation when running in the full speed counter-rotating direction. This condition provides considerable additional command torque authority for accelerating the wheel even when running at or near full design speed.

### Induction Motor

Number of Poles	- 30
Operating Speed	- 0 to $\pm 167.5$ rad/s ( $\pm 1600$ rpm) maximum;

Table 2.5-1  
Calculated Nominal Performance

System Angular Momentum, H, N-m-s	-7.51	+176	+7.86
Middle Spin Element Speed, rad/sec	+ 335	+ 335	+ 335
Wheel Speed, rad/sec	-167.5	0	-167.5
<u>Inner Bearing</u>			
Axial Stiffness, $\left(K_a\right)_1, 10^8 \text{ N/m}$	0.750	0.750	0.750
Safety Factor	3.4	3.4	0.4
Radial Stiffness, $\left(K_r\right)_1, 10^8 \text{ N/m}$	1.03	1.03	1.03
Safety Factor	4.5	4.5	4.5
Angular Stiffness $\left(K_\theta\right)_1, 10^5 \text{ m-N/rad}$	0.89	0.89	0.89
Safety Factor	12.8	12.8	12.8
<u>Outer Bearing</u>			
Axial Stiffness, $\left(K_a\right)_o, 10^8 \text{ N/m}$	0.804	0.554	0.303
Safety Factor	4.8	3.3	1.8
Radial Stiffness, $\left(K_r\right)_o, 10^8 \text{ N/m}$	2.31	1.72	1.06
Safety Factor	10.2	7.6	4.7
Angular Stiffness, $\left(K_\theta\right)_o, 10^5 \text{ m-N/rad}$	2.15	1.42	0.89
Safety Factor	23.8	15.6	10.0
<u>System Stability</u>			
Critical Mass, $\left(M_{cr}\right)_r, \text{ N-s}^2/\text{m}$	333	164	64.5
Actual Mass, $M_M + M_W, \text{ N-s}^2/\text{m}$	3.68	3.68	3.68
Safety Factor	89	44	17
Critical Inertia, $\left(I_{cr}\right)_r, \text{ N-m-s}^2$	0.42	0.20	0.055
Actual Inertia, $I_W + I_M, \text{ N-m-s}^2$	0.023	0.023	0.023
Safety Factor	18.5	8.6	2.4
<u>System Power Loss</u>			
Inner Bearing Power Loss, $P_i, \text{ watts}$	3.8	3.8	3.8
Outer Bearing Power Loss, $P_o, \text{ watts}$	22.5	10.0	7.5
Windage Loss, $P_{\text{windage}}, \text{ watts}$	1.0	0	1.0
Total System Power Loss, watts	27.3	13.8	12.3
<u>Drive Power Required</u>			
From Middle Spin Element Motor, $P_M, \text{ watts}$	18.8	13.8	8.8
From Wheel Motor, $P_W, \text{ watts}$	8.5	0	3.5
Total, $P_M + P_W, \text{ watts}$	27.3	13.8	12.3

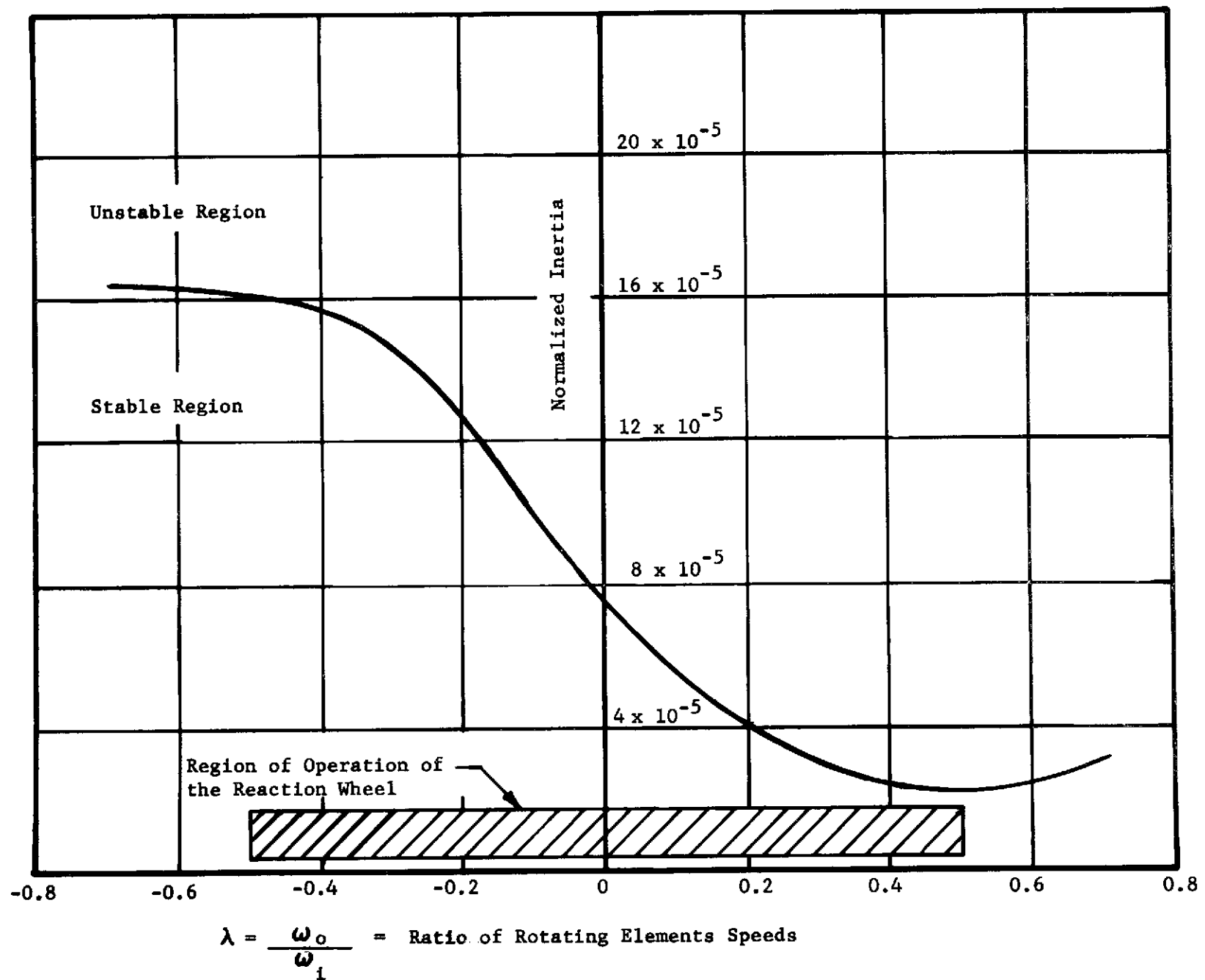


Figure 2.5-1 Stability Map for Angular Motions of the Rotating Assembly

Load Torque Capability	- 0.120 N-m (17 oz-in.) at $\pm 167.5$ rad/sec (1600 rpm);
Stall Torque	- 0.226 N-m (32 oz-in.) momentary over-voltage excitation permissible);
Acceleration Torque	- 0.261 N-m (37 oz-in.) momentary at $\pm 167.5$ rad/s (1600 rpm); with overvoltage excitation permitted;
Excitation	- two-phase 800 Hz, 35V rms sinewave both phases at 167.5 rad/s (1600 rpm).

The two stator stacks are shrunk into a single aluminum housing that bolts directly to the reaction wheel case near the mounting flange, affording a good head conductive path to the outside. The induction rotor is an electrical steel alloy, electron beam welded on an Inconel X750 substrate on the outer rim of the reaction hub. Similarly, the laminated hysteresis ring is attached to an Inconel rotor which is piloted and fastened with screws to the middle spin element.

## 2.7 Materials

The material used for the precision bearing parts is I400 beryllium, the choice being dictated by thermal considerations. Thermal distortions are minimized by the use of Be, because of the low value of  $\alpha/k^*$ . This promotes much more uniform temperatures in the bearing regions, and smaller relative deformations of the film shape than would be the case with aluminum or steel. Other parts of the wheel are fabricated from conventional materials. The inertia ring is 416 stainless steel, and the other major parts are various aluminum alloys.

## 2.8 Fabrication of Precision Bearing Parts

Fabrication of the spherical bearing components is the only part of the reaction wheel that requires special manufacturing techniques. These parts have extremely close tolerances specified and require very special tooling and fixtures.

The bearing is made up of five parts: two opposed hemispherical stators, two opposed hemispherical intermediate spin element rotors, and a single outer hub with opposed hemispherical inner surfaces. Each of these parts is rough machined and heat-treated. Semifinish machining is then done, and mating surfaces are nickel plated. The plating provides a hard surface that

-----

\*  $\alpha$  = coefficient of thermal expansion

k = thermal conductivity

can be lapped to set the exact center distance of the opposed hemispheres and align their axes of rotation. Further, it avoids butting the plasma-sprayed chrome oxide edges that might result in cracking or chipping. At this point, the spherical surfaces are  $7.62 \times 10^{-5}$  m (0.003 in.) undersize or oversize, depending on whether it is convex or concave, respectively. The spherical surfaces are then plasma-sprayed with chrome oxide and rough-ground to size.

Final grinding is to size, except for sufficient stock to lap into the required tolerance. This final lapping operation includes lapping of critical faces, diameters, and spherical radii to set required clearances between mating bearing components. Parts are then inspected and measurements made to determine the exact size of each. These data are then used to calculate the axial and radial shape to be expected at assembly. Following inspection, the appropriate parts have the spiral grooves applied to their surfaces, after which they are ready for assembly and balancing.

#### Generation of Spiral Grooves

Sputter-etching of the bearing provided uniform and well defined reproducible grooves. Depths were maintained to a tolerance of about 5  $\mu$  in. along the groove, and from one groove to another. Etching rates of about  $7.0 \times 10^{-12}$  m/s (10 micro in./hr) were used at power rates that do not cause excessive heating.

Before assembly bearing interface surfaces received a coat of steramide, a lubricant to enhance the starting forces by decreasing the touchdown stiction.

Bearing assembly is one of the most critical and difficult parts of the fabrication task. The one-piece outer hub dictates blind assembly of the two halves of the middle spin element. This procedure is accomplished by chilling the locating ring that mates the two parts, and pressing both onto the ring. Assembly of the two parts on the ring is accomplished in two separate operations. Since the shrink fit on the ring is not exceptionally tight (to avoid distorting bearing surfaces), parts are prevented from operating on the ring by spot applications of epoxy. The parts are then checked for proper assembly by precise height measurements and comparison with previous data taken in trial assembly where the outer hub was not involved. This, of course, must all be done in the strictest clean room conditions.

### 3.0 TESTS

#### 3.1 Summary of Tests After Assembly

The instrumentation for tests performed after assembly at MTI is set forth in a block diagram in Figure 3.1-1. In addition to this instrumentation, the bearing performance, i.e., orbit of displacement from a state of equal and symmetrical clearances, was measured by a set of capacitance-type pickup probes and the orbits of both rotating elements were displayed upon oscilloscopes.

##### Bearing Orbit Measurement

The bearing orbit observed on an oscilloscope is a fundamental measurement of the quality of the bearing. Before test, 50% of the bearing film thickness was considered acceptable performance as a maximum to be applied to the orbit parameter. (100% of the bearing film thickness would constitute touching of the bearing surface.) 50% of the film relates to  $1.91 \times 10^{-6}\text{m}$  (75  $\mu\text{in.}$ ). Total deviation observed in the monitored tests at MTI were less than  $0.254 \times 10^{-6}\text{m}$  (10  $\mu\text{in.}$ ) with the bearing spin rotation axis both vertical and horizontal. Therefore, the actual tests surpassed the acceptable criteria by greater than a factor of 7.

While the reaction wheel was rotated at  $\pm 0.052 \text{ rad/sec}$  ( $3^\circ/\text{sec}$ ), bearing orbit resulted in nondetectable orbit measurements, except in the maximum "co-rotating" state. In this condition a deviation of  $1.524 \times 10^{-6}\text{m}$  (60 micro in.) was observed, also well under the prescribed criteria.

##### Power versus Speed Measurement

The specification requires that the bearing design exhibit a combined inner and outer bearing power loss not to exceed 3.77 watt/N-m-s (5 watts/ft-lb sec) of maximum design angular momentum. This wheel has a minimum of 6.8 N-m-s (5 ft-lb sec) angular momentum at full speed; therefore the bearing power losses must not exceed 25 watts. The measured bearing power losses at 167.5 rad/sec (1600 rpm) counter-rotating (worst case) are 20.15 watts, of which 14.92 are supplied by the inner motor, and 5.22 by the outer motor.

##### Temperature Measurements

Maximum temperature rise observed to a steady state condition was  $17^\circ\text{C}$  ( $30^\circ\text{F}$ ) [from room ambient of  $34^\circ\text{C}$  ( $60^\circ\text{F}$ ) to  $51^\circ\text{C}$  ( $90^\circ\text{F}$ )], which occurred near the inner bearing surfaces on both the motor end and encoder end.

##### Liftoff/Touchdown Characteristics

- 1) 15 to 20 rad/sec ( $\approx 150$  to 200 rpm) by observation of tachometer on outer element;
- 2) 12 to 15 rad/sec ( $\approx 120$  to 150 rpm) liftoff on inner as recorded from probe data.

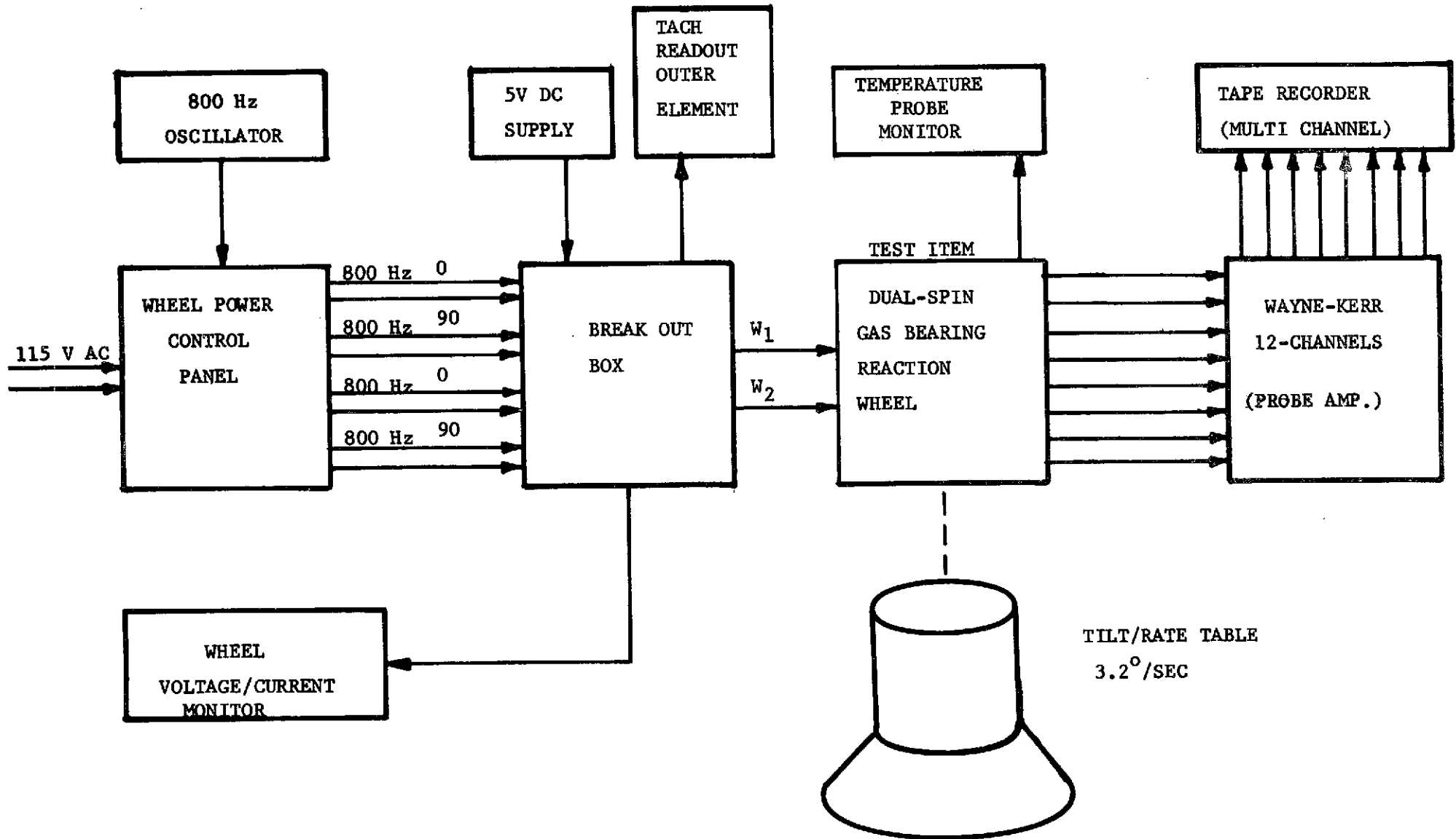


Figure 3.1-1 Block Diagram of Test Setup

### 3.2 Acceptance Tests

The acceptance test documentation is provided in Appendix A of this report.

### 4.0 CONCLUSIONS AND RECOMMENDATIONS

Fabrication of the dual spin gas bearing reaction wheel provides additional proof that a low torque noise, i.e., zero stiction reaction wheel is realizable for long-life space missions with gas bearing technology. The dual spin gas bearing reaction wheel, the second reaction wheel built to the previously established design, is proof the concept has been further confirmed. The potential of this technology is in control systems for fine pointing applications, e.g., the Large Space Telescope. The long-life characteristics of the gas bearing provides a technically feasible device for a ten-year life objective.

During fabrication of the dual spin reaction wheel, there developed several areas where the margin of performance could be enhanced by further design effort. The electrical motor could be improved by further design of the motor element. The motor torque for the middle spin element was marginal (for one-g earth tests) and a design improvement for lower axial forces on the rotor may be desirable. Lubrication applied to the bearing surfaces to decrease touchdown start forces could also be the subject of further design effort. The first unit fabricated and tested was lubricated with lithium stearate. With repeated starts/stops, the lubricant was physically scrubbed away and accumulated in the spiral grooves towards the bearing center, contributing to uneven and excess friction. Because of multiple assembly/disassembly operations, two coatings of lithium stearates were applied and this could have resulted in excessive buildup partially accounting for the problem. The NASA unit was lubricated with steramide which, although representing an improvement over lithium stearate, may not be the most favorable choice. It should be mentioned that space application does not involve the forces of a one-g earth's test environment, and some of the marginal characteristics in testing on earth are non-existent in the orbital application.

The dual spin gas bearing reaction wheel design has passed the proof of concept phase, and represents a development state acceptable for future application in a space vehicle system.



APPENDIX "A"

---

ACCEPTANCE TEST REPORT

AND

OPERATING PROCEDURE FOR

DUAL SPIN GAS BEARING  
REACTION WHEEL

MARTIN MARIETTA CORPORATION  
P. O. Box 179  
Denver, Colorado 80201

PRECEDING PAGE BLANK NOT FILMED

FINAL REPORT

MTI 74TR2

DUAL SPIN REACTION WHEEL

PERFORMANCE TESTS

Item 2: The NASA Wheel

by

J.T. McCabe  
B.F. Geren

November 1973

Prepared for

Martin-Marietta Corporation  
Denver Division  
Denver, Colorado

Prepared under

Contract AC2-410024

MECHANICAL TECHNOLOGY INCORPORATED  
968 Albany-Shaker Road  
Latham, New York 12110

TABLE OF CONTENTS

	<u>Page</u>
FOREWORD-----	iv
INTRODUCTION-----	1
SUMMARY-----	2
RECOMMENDATIONS-----	3
TEST PROCEDURES AND RESULTS-----	4
Instrumentation Description-----	4
Types of Tests-----	5
APPENDIX A - STARTING AND STOPPING PROCEDURES-----	14

FOREWORD

This program was conducted under Contract RC2-410024 for the Advanced Guidance and Control Section of the Martin Marietta Electronics Research Department with Mr. Sid Wright acting as Technical Monitor. The work was performed by the Advanced Machinery Development Center of the Mechanical Technology Incorporated Advanced Technology Department. Mr. J.T. McCabe acted as Program Manager for MTI.

## I. INTRODUCTION

The dual spin reaction wheel here described is a new concept that permits precise control of angular momentum within the range -5.8 ft-lb-sec to +6.1 ft-lb-sec. Variation of the angular momentum is accomplished by an inertia ring mounted on an outer rotor that can be driven from zero to 1600 rpm in either direction by an induction motor. Bearing support for the outer rotor is provided by a hydrodynamic gas film generated by spiral grooves that are ion-machined into an intermediate rotor. The intermediate rotor consists of two hollow hemispheres that are truncated, joined at the pole-faces and driven at a constant speed of 3200 rpm by a synchronous hysteresis motor. Support for the intermediate rotor is provided by spherical hydrodynamic gas bearings fitted onto a stationary shaft.

MTI report 71TR60 prepared under MMC Contract RCl-201-097 describes an analytical comparison study of potential bearing geometries and recommends the spherical configuration. In August 1972, an interim report entitled, "Design of Dual-Spin, Gas Bearing Reaction Wheel," was issued to MMC. The interim report presents a complete description of the theoretical performance predictions including the following:

- Gas bearing design criteria
- Bearing stiffness, friction and stability data
- Estimation of windage losses and starting torque requirement
- Thermal maps of the bearing region
- Stress and deformation calculations
- A summary of system natural frequencies

Two reaction wheels were fabricated and tested. One is here referred to as the IRAD Wheel, the other is called the NASA Wheel. This report is primarily concerned with performance tests of the NASA Wheel and contains the following:

- A summary of important findings based on the fabrication and testing of both wheels
- Recommendations for improving the design implementation of the dual spin reaction wheel concept
- Test procedures and results
- Starting and stopping procedures (Appendix A)

This report, together with a set of design drawings that have been forwarded under separate cover, constitutes fulfillment of the Task 4 — Documentation requirement for the NASA Wheel as specified in Exhibit A of MMC Statement of Work 72-48181-3.

## II SUMMARY

The program has demonstrated the following:

- The dual spin reaction wheel concept is feasible.
- Two reaction wheels were fabricated and tested and their measured operating characteristics were virtually the same.
- The bearing and rotor dynamic characteristics were in good agreement with theoretical predictions.
- The calculated angular momentum at the maximum test speed of 1600 rpm was 6.17 ft-lb-sec in co-rotation and 5.81 ft-lb-sec in counter-rotation.
- Test on both wheels showed the maximum start-up torque provided by the hysteresis motor is marginal for the present design in a 1 g environment.
- The maximum available voltage of about 53 volts was required to start the hysteresis motor with spin axis vertical; 20 volts was found to be a safe normal operating level and synchronous speed dropout occurred between 6 and 7 volts.
- The induction motors had adequate start-up torque safety margin.
- Tests indicate the present design would perform well if started and operated in a zero g environment.
- About 25 percent more motor torque was required for startup with spin axis vertical than with spin axis horizontal.
- A significant percent of the manufacturing time was devoted to learning techniques for plasma spraying, grinding, lapping and measuring the nested spherical surfaces required for this particular application.
- Except for the initial cost associated with bearing manufacturing techniques, there is no apparent intrinsic disadvantage associated with the spherical bearing geometry.

### III RECOMMENDATIONS

- To improve start-up reliability, either the weight of the rotating assembly should be reduced by a factor of two or the starting torque of the synchronous motor should be increased by a factor of two. The latter must be accomplished without a substantial increase in the unbalanced electromagnetic force.
- Sputter-deposited  $\text{MoS}_2$  should be investigated as a boundary lubricant for the reaction wheel.
- Based on observed interrelationships among design, manufacture and performance tests, a second generation gas bearing reaction wheel should be constructed to demonstrate improvements in power consumption, weight reduction, start-up reliability and manufacturing simplification that are now apparent.

#### IV. TEST PROCEDURES AND RESULTS

##### 4.1 Instrumentation Description

- Radial and axial motions of the outer and intermediate rotating assemblies were monitored by ten capacitance probes.
- The capacitance probe outputs were displayed on oscilloscopes and recorded on magnetic tape.
- Speed of the intermediate rotor was intermittently monitored by a stroboscope.
- Speed of the outer rotor was continuously monitored by a counter driven by the encoder output voltage.
- Temperature of the inner bearing was intermittently monitored by a thermocouple potentiometer display.
- Voltage inputs to the induction and synchronous motors were displayed on digital voltmeters.
- The current through one phase of each motor was displayed on an ammeter.
- A voice track on the magnetic tape was provided for the test engineer.
- Probe target positions and calibrations were as follows:

<u>Probe No.</u>	<u>Position</u>	<u>Calibration mils/volt.</u>
	<u>Outer Spin Element</u>	
1*	Encoder end, Radial, Vertical	5.146
6*	Encoder end, Radial, Horizontal	5.047
8	Encoder end, Axial	5.469
11	Encoder end, Axial	5.159

\* Mechanical runout of probe 4 and 6 target was 80 mv peak-to-peak once-per-revolution and 20 mv peak-to-peak twice-per-revolution. This distortion probably occurred when the induction motor ring was plated.



<u>Probe No.</u>	<u>Position</u>	<u>Calibration mils/volt.</u>
<u>Intermediate Spin Element</u>		
3	Encoder end, Radial, Vertical	5.070
4	Encoder end, Radial, Horizontal	5.442
2	Motor end, Radial, Vertical	5.461
5	Motor end, Radial, Horizontal	5.298
10	Encoder end, Axial	5.150
12	Encoder end, Axial	5.174

#### 4.2 Types of Tests

The following types of tests were conducted:

- Displacement tests of inner and outer rotors at zero speed
- Dynamic bench tests without inertia ring
- Static breakaway tests
- Dynamic bench tests with inertia ring
- Rate tests

##### 4.2.1 Displacement Tests

The outer rotor, consisting of the hub assembly, encoder disc assembly and outer bearing were moved by hand to determine the bounds for axial and radial displacement and the locus of each was traced on oscilloscope monitor faces. During this test, the inner rotor was not restrained. Next, the inner rotor was moved by hand and the displacement bounds were traced on the appropriate oscilloscopes. All trace envelope dimensions were found to be in good agreement with calculated values based on hardware inspection reports and probe calibration data.

##### 4.2.2 Dynamic Bench Tests Without Inertia Ring

The measured weights of the rotating assemblies were:

Outer rotor assembly less inertia ring = 36.34 oz.

Inner rotor assembly = 20.80 oz.

The wheel was mounted with spin axis vertical and started by the counter rotation procedure. This procedure consists of applying motor torque to

restrain the inner rotor from movement until a gas bearing film is developed at the outer bearing by the counter rotating induction motor, then increasing the hysteresis motor voltage until a film is developed at the inner bearing, see Appendix A. After successfully developing a gas bearing film in all bearings, the unit was shutdown by first ramping the hysteresis motor voltage to zero, waiting several seconds for the intermediate rotor to stop, then ramping the induction motor voltage to zero. Scope patterns for this run indicated normal performance compared to past experience with the previously tested MMC IRAD wheel.

The wheel was again started in counter-rotation with spin axis vertical and the breakaway voltage for the hysteresis was recorded at 34 v, as shown on Table 1 for test dated 11/2/73 (0). Motor performance curves, not presented here, show 34 v corresponds to a stall torque of 14.73 in. oz., which was considered high based on the weight of the elements and the surface friction coefficient.

The outer rotor speed versus induction motor input voltage was recorded with spin axis vertical and, with the unit still running, the test bench was tilted to spin axis horizontal and similar data was recorded. This data is given in Figure 1 which also shows the comparable curve taken for the IRAD wheel. These curves show the two units performed essentially in a similar manner. Discrepancies between the two curves reflect slight difference in bearing clearances due to manufacturing tolerances.

These tests indicated that when the inertia ring was installed, the wheel should exhibit satisfactory dynamic performance as did the previously tested IRAD Wheel.

#### 4.2.3 Static Break-away Tests

The inertia ring, weighing 77.07 oz. with mounting screws, was attached to the hub assembly, bringing the total weight of the outer rotating assembly to 113.41 oz. A Mylar tape was wrapped around the 14" OD of the inertia

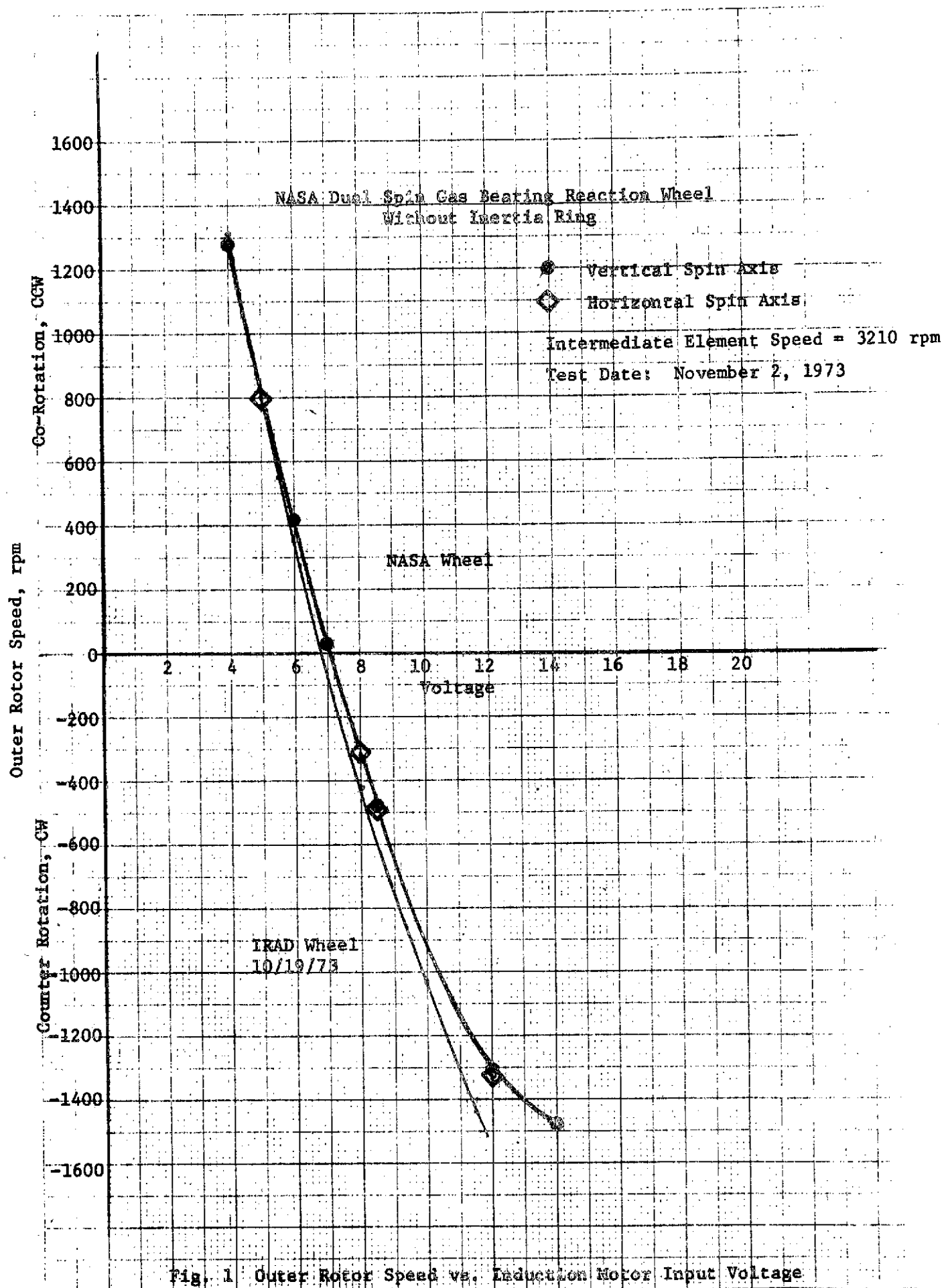
TABLE 1  
BREAKAWAY VOLTAGE AND CURRENT PER PHASE FOR NASA  
DUAL SPIN GAS BEARING REACTION WHEEL

<u>Date</u>	<u>Position Spin Axis</u>	<u>Synchronous Motor Intermediate Bearing</u>		<u>Induction Motor Outer Bearing</u>	
		<u>Volts</u>	<u>Amps</u>	<u>Volts</u>	<u>Amps</u>
11/2/73 (0)	W/O Rim Vertical	34	1.3	15	1.5
11/2/73 (1)	Vertical	46.9	---	40.0	---
(2)	Vertical	46.0	---	43.0	---
(3)	Vertical	47.0	---	40.0	---
(4)	Vertical	41.0	---	60.0 <sup>+</sup>	---
11/5/73 (1)	Horizontal	60.0 <sup>+</sup>	1.8	32.0	2.4
(2)	Horizontal	60.0 <sup>+</sup>	2.0	36.0	2.9
(3)	Horizontal	61.0 <sup>+</sup>	3.0	36.5	2.0
(4)	Horizontal	61.0 <sup>+</sup>	2.7	34.0	2.9
11/6/73 (1)*	Horizontal	72.0 <sup>+</sup>	3.25	37.0	3.2
(2)**	Horizontal	72.0 <sup>+</sup>	3.30	37.0	3.2

\*Intermediate spin element did not start. Helium pressure was 0 psig.

\*\*Helium pressure was 6.5 psig.

+Maximum voltage from power supply is 53 volts; Values recorded in excess of 53 volts are due to distortion in power supply.



ring and attached to a spring scale. With spin axis vertical, the breakaway torque between the inner and intermediate bearing was measured at 16.8 in.oz., which corresponds to a stall torque voltage of 37 v for the synchronous motor.

The breakaway torque between the intermediate and outer bearing was measured at 28.0 in.oz. which corresponds to a stall torque voltage of 29.5 v for the induction motor.

Since the measured stall torque of the synchronous motor exceeded 30 in. oz., and the induction motor stall torque exceeded 50 in. oz., the measured breakaway torques were considered satisfactory. In addition, the friction coefficients computed from the measured data were in good agreement with previous theoretical predictions.

#### 4.2.4 Dynamic Bench Tests With Inertia Ring

As shown on Table 1, the wheel was started four times with spin axis vertical and five times with spin axis horizontal. During all start-ups, both DC power supplies were set at 37.5 v per MMC instructions and, according to MMC personnel, the maximum possible motor input voltage was the product of  $\sqrt{2}$  and the DC power supply voltage setting. Thus, voltages on Table 1 in excess of 53 v were probably due to distortion in the power supply and should be taken as the maximum value of 53 volts.

The start-up voltage of 46.9 v for test dated 11/2/73 (1) corresponds to a hysteresis motor stall torque of 27.4 in.oz., which was significantly higher than the breakaway torque of 16.8 in.oz. measured mechanically as described in Section 4.2.3. Since the measured maximum stall torque for the hysteresis motor was about three inch ounces greater than the stall torque required to start the inner rotor, the influence of unbalanced electromagnetic force on the breakaway torque requirement was significant in this design. The presence of a significant unbalanced electromagnetic force was observed on the oscilloscope as a radial displacement of the middle spin element that increased to the limit of the bearing clearance as the hysteresis motor input voltage was increased. The effect of unbalanced electromagnetic force on start-up should be explored in future tests.

Table 2 shows motor input voltage and current per motor phase versus speed of the wheel. Assuming the motor power input is twice the per phase measurements, then the total power input was 70.6 watts at -1600 rpm, 43.1 watts at 0 rpm and 40.8 watts at + 1600 rpm. Windage loss was estimated to be about 1.1 watts at 1600 rpm.

Figure 2 shows a plot of the wheel speed versus the induction motor input voltage per phase. At + 1600 rpm the angular momentum was calculated to be 6.1 ft. lb. sec; at -1600 rpm the angular momentum was calculated to be 5.8 ft. lb. sec.

The wheel was next mounted on a tilt table with spin axis vertical and run at wheel speeds of +1600, 0 and -1600 rpm. Axial and radial positions of both rotors were recorded on magnetic tape. The spin axis was tilted to 41.5°, 60°, 75.5° and 90° relative to horizontal. At each inclination, the three extreme wheel speeds were repeated and position data was recorded on magnetic tape. Based on this data, bearing stiffnesses in lb/in. were estimated as follows:

<u>Wheel Speed</u> <u>rpm</u>	<u>Axial Stiffness</u>		<u>Radial Stiffness</u>	
	<u>Inner Film</u>	<u>Outer Film</u>	<u>Inner Film</u>	<u>Outer Film</u>
+1600	380,000	35,000	200,000	58,000
-1600	380,000	101,000	200,000	126,000

#### 4.2.5 Rate Tests

The final tests consisted of operating the wheel on a rate table. The spin axis of the wheel was horizontal and the spin axis of the rate table passed through the center of the wheel. The wheel speed was fixed at +1600 rpm and the rate table was driven at 3 degrees per second. Wheel orbits were recorded on magnetic tape. This test was repeated for wheel speeds of 0 and -1600 rpm. The maximum displacement recorded by the capacitance probes occurred in the co-rotation mode at 1600 rpm and was about 60 micro-inches, or about 1/3 of the bearing clearance. Displacement at other wheel speeds were small in comparison to the detection circuit noise level.

The maximum temperature measured during any of the dynamic tests was 83°F in a room ambient temperature of 67°F.

TABLE 2  
INDUCTION MOTOR INPUT FOR NASA DUAL  
SPIN GAS BEARING REACTION WHEEL

Intermediate Spin Element Speed = 3210 RPM  
at 36 Volts and .5 Amps

Ambient gas: Helium at 6.5 psig and 90° F

	<u>WHEEL SPEED</u>	<u>INDUCTION MOTOR</u>	
	<u>RPM</u>	<u>Voltage</u>	<u>Amps</u>
Counter Rotation	- 1600	16.6	1.05
	- 1350	14.1	.95
	- 1150	12.5	.85
	- 480	9.0	.7
	- 450	8.9	.7
	0	7.1	≈ .5
	800	4.2	----
	1222	1.7	----
	1282	1.0	----
	1319	.6	----
Co-rotation	1351	- 1.2	----
	1425	- 3.6	----
	1520	- 4.6	≈ .1
	1600	- 6.1	≈ .1

Notes:

- (1) Wheel speed of -1600 rpm corresponds to a computed angular momentum of 5.81 ft-lb-sec
- (2) Wheel speed of +1600 rpm corresponds to a computed angular momentum of 6.17 ft-lb-sec
- (3) Voltage and Amps are given per phase

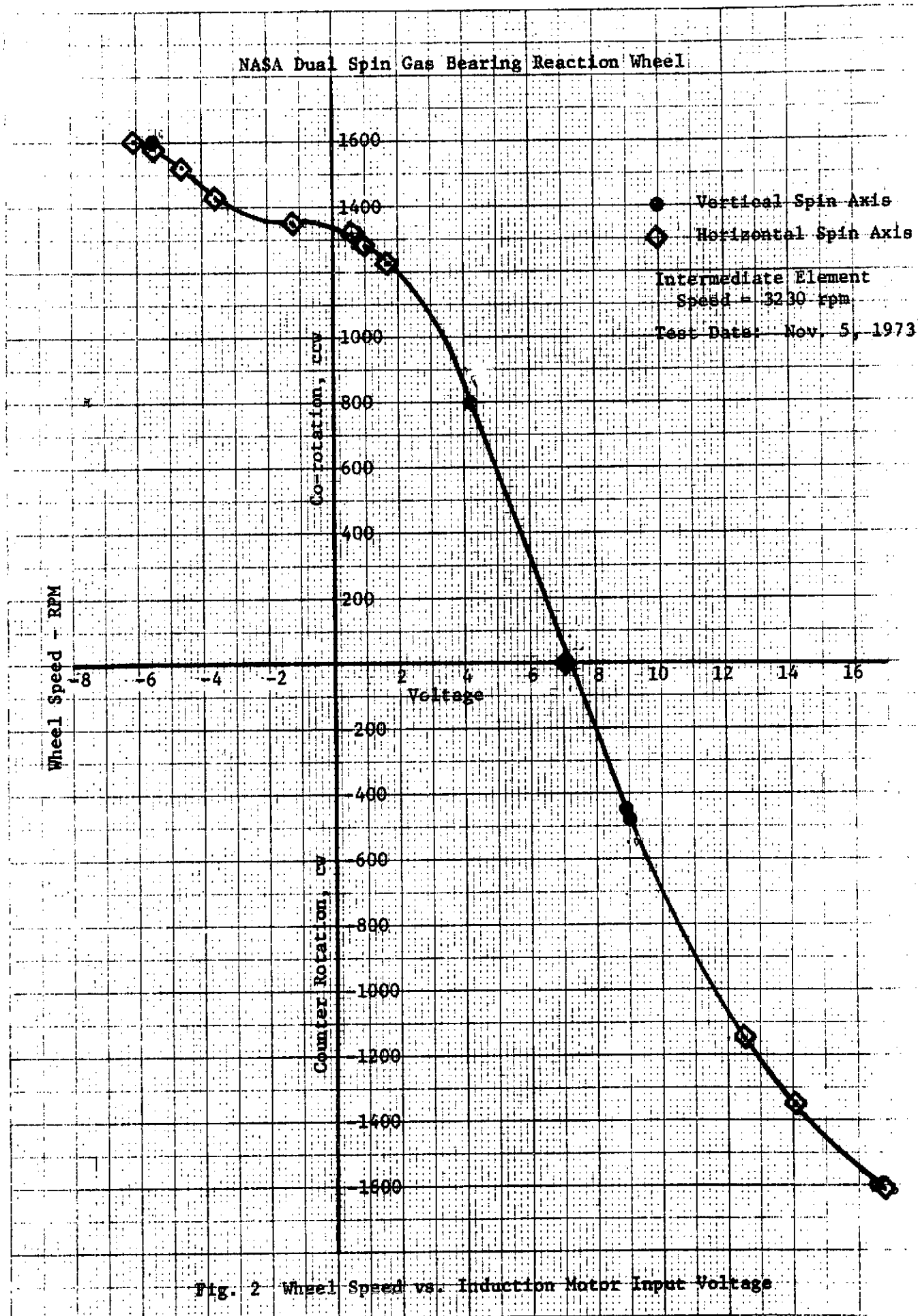


Fig. 2 Wheel Speed vs. Induction Motor Input Voltage



In summary, all tests performed indicated ample safety margins in stability and minimum film thickness over the design speed range. One problem area was encountered and that concerned the start-up reliability of the hysteresis motor.

APPENDIX A  
STARTING AND STOPPING PROCEDURES  
FOR DUAL SPIN REACTION WHEEL

A.1 Counter-Rotation Start-Up Procedure

- a. Preset voltage on synchronous motor (intermediate spin element) to 30 volts.
- b. Apply voltage to induction motor (outer spin element) for the counter rotation direction. Lift-off will occur between 45 to 53 volts with spin axis vertical; with the spin axis horizontal, lift-off will occur between 35 and 40 volts.

While applying voltage to the induction motor, monitor the intermediate spin element. If it starts to rotate in the clockwise direction, increase voltage to the synchronous motor to hold it in place.

- c. Adjust voltage of induction motor until outer spin element is between 400 to 500 rpm with the spin axis either vertical or horizontal. Therefore the safe minimum speed of the outer element at this point in the starting procedure is 250 rpm.
- d. Increase voltage to the synchronous motor (intermediate spin element) until it lifts off. The power requirements will probably be full capacity of the synchronous motor. As soon as the synchronous motor is in sync., reduce voltage to 25+5 volts.

Table 1 is a tabulation of the starting power requirements in counter-rotation for the NASA Reaction Wheel during the MTI testing phase.

A.2 Shutdown Procedures

- a. With the outer spin element in the counter-rotation mode and at a speed of 350+50 rpm, turn off the power to the synchronous motor by ramping the voltage to zero. The synchronous motor will drop out of sync between 6 to 8 volts. The coast down time for its intermediate spin element is approximately 10 seconds. When the intermediate spin element stops, the outer spin element will gradually increase in speed.

- b. As soon as possible, turn off the power to the induction motor (outer spin element) by ramping the voltage to zero. The coast-down rate for the outer spin element is approximately 6 rpm per second. Film collapse will occur at approximately 175 to 200 rpm

APPENDIX "B"

---

DRAWING LIST

MARTIN MARLETTA CORPORATION  
P. O. Box 179  
Denver, Colorado 80201

DRAWING LIST

MTI NUMBER	REVISION	TITLE
275 E03	D	Bearing Housing
275 E04	C	Assembly, Gas Bearing Reaction Wheel
275 D05	D	Bearing, Spherical, Inner
275 D06	D	Bearing, Spherical, Intermediate
275 D07	E	Bearing, Spherical, Outer
275 E08	A	Inertia Ring
275 E09	B	Cover, Development
275 D11	D	Hub & Ring Assembly, Outer Bearing
275 C12	-	Ring
275 C13	B	Ring, Induction Motor
275 C14	-	Ring, Holder, Glass Disc
275 C15	D	Ring, Motor, Hysteresis
275 C16	-	Bracket, Encoder
275 D17	C	Bracket, Probes and Encoder
275 C18	-	Bracket, Probe
275 D21	D	Hub and Bearing Assembly
275 C22	-	Gasket
275 D23	-	Hub, Outer Bearing
275 C26	-	Shim
275 C27	A	Shaft
275 C28	A	Ring, Locating
275 B29	-	Encoder Bracket
275 B33	-	Shaft Nut and Washer
275 D34	A	Assembly for Bearing Clearance Measure- ment
275 D35	-	Shaft & Bearing Housing Assembly
<u>SCHAEFFER</u>		
<u>MAGNETICS NO</u>		
100985	A	Motor Set, Induction & Hysteresis Synchronous

APPENDIX "C"

---

SPECIFICATION

FOR

DUAL SPIN GAS BEARING  
REACTION WHEEL

MARTIN MARIETTA CORPORATION  
P. O. Box 179  
Denver, Colorado 80201

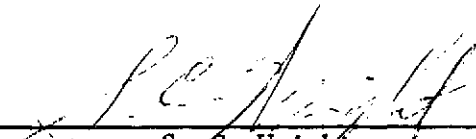
REVISION A (3.1.1) - 4/5/72  
REVISION B - 11/8/72


72-48181-4  
C-1

DESIGN CRITERIA - REACTION WHEEL

LAB 2999205

Prepared by:

  
S. C. Wright

  
R. L. Gates

Advanced Guidance and Control,  
and Space Power Section 1625  
Electronics Research Department

MARTIN MARIETTA CORPORATION  
DENVER DIVISION  
P. O. Box 179  
Denver, Colorado 80201

## 1.0 SCOPE

### 1.1 Purpose:

The purpose of this document is to define the design and performance requirements for a dual-spin gas-bearing reaction wheel, and to describe the environmental conditions which it is expected to survive and under which it must operate. The reaction wheel will be used as a momentum exchange control element in spacecraft attitude control systems. The dual-spin gas-bearing concept makes possible a long operating life, and has the further advantage of essentially stictionless operation around zero-speed and infinite resolution at any speed. With these attributes its application will be that of a "fine pointing" actuator for long duration earth orbit and planetary missions.

## 2.0 APPLICABLE DOCUMENTS

The reaction wheel design shall conform to the extent specified herein to the requirements of the following documents. If a conflict exists between the requirements of this design criterion and any document referenced herein, the requirements of this design criterion shall take precedence.

MIL-STD-100A	Engineering Drawing Practices
MS 24123A	Plate, Identification
NASA 40M39569B	Connectors, Electrical

## 3.0 REQUIREMENTS

### 3.1 Design Requirements

3.1.1 Bearing Design - The bearing shall be a dual-spin hydrodynamic design. Bearing surfaces shall be spherical, with spiral pumping grooves.

The bearing shall consist of three parts: An inner element or stator, a middle-spin element driven at constant speed, and an outer element which carries the inertia rim and may be driven at varying speeds in either direction from zero to design maximum. When operating, the elements of the bearing shall remain stable over the design speed range of the outer element running in either direction, and when subjected to either a one-g or a zero-g gravitational force and angular rates about any axis up to  $\pm 3$  degrees per-second.

The bearing material for the inner element and the middle spin element shall be beryllium with a plasma sprayed chromium oxide finish. The material for the outer spin element may be other than beryllium to obtain higher inertia at reasonable speeds, and its bearing surface finish shall be selected to meet the start-stop requirements of 3.2.4.3.



The bearing design shall be such as to permit substitution of motors if required for model variations having different design maximum angular momentums as specified in 3.1.2. This may be accomplished by designing to accept adaptor discs with a common inner diameter, and various outside diameters to fit different size motor bores.

For purposes of definition in these criteria, the interface between the inner element or stator and the middle spin element will be referred to as the inner bearing. The interface between the middle spin element and the outer element will be referred to as the outer bearing.

3.1.2 Angular Momentum Range - The design of the bearing shall permit model variations having maximum angular momentums for the outer element over the range 0.55 to 5.5 ft-lb-sec in the co-rotational mode. The angular momentum of the middle spin element (exclusive of motor parts) shall be minimized, and when operating at design speed shall in no case exceed 5 percent of the maximum angular momentum of the outer element.

### 3.1.3 Drive Motors

3.1.3.1 Middle Spin Element Motor - The middle spin element drive may be one or two motors depending on design trades between starting torque, reliability, running efficiency, the benefits of symmetry, etc. The motor(s) shall be synchronous hysteresis motors which have the following electrical characteristics:

Motor Characteristics      TBS

3.1.1.2 Outer Element Motor - The outer element drive may be one or two motor depending on design trades between running efficiency, reliability, torque margin at maximum design speed, the benefits of symmetry, etc. The motors shall be variable speed induction motors having the following electrical characteristics:

Motor Characteristics      TBS

3.1.4 Tachometer - A tachometer mechanization capable of measuring the relative rotational rates between the outer element and the reaction wheel case is required. Slip rings or brushes are not permitted as a part of the tachometer mechanization. The tachometer shall have the following characteristics:

Tachometer Characteristics      TBS

3.1.5 Mounting Provisions - The reaction wheel case mounting design shall be such as to support the reaction wheel and maintain its alignment while being subjected to any combination of the environments of paragraph 3.3. The case mount shall also serve as the alignment reference, and shall define the spin axis of the reaction wheel to an accuracy of 1.0 arc-minute. The case mount shall also be the only thermally conducting path (exclusive of wiring) to the structure to which the reaction wheel is attached.

3.1.6 Weight - The design shall minimize the weight to angular momentum ratio, and in no case shall exceed TBS lbs for the 0.5 ft-lb-sec, and TBS lbs for the 5.0 ft-lb-sec wheel.

3.1.7 Electrical Connections - All electrical connections to the reaction wheel (except development instrumentation) shall be made through a single electrical connector conforming to the requirements of NASA 40M39569B.

3.1.8 Phasing - TBS

3.1.9 Surface Finish - The surface finish shall serve as control for the radiation and/or absorption of heat, and shall be selected to meet the requirements of the stated environments.

### 3.2 PERFORMANCE REQUIREMENTS

3.2.1 Stability - The reaction wheel shall exhibit stability over the full momentum range (including start-up) when operating at any orientation in either a zero- or one-g field.

3.2.2 Reaction Wheel Body Rates - The bearing design shall be such that neither touchdown nor instabilities occur when rates as high as  $\pm 3$  degrees per-second exist about an axis normal to the spin axis of the momentum wheel for any value of the design momentum range.

3.2.3 Bearing and Windage Losses - The reaction wheel shall be designed such that the combined inner and outer bearing losses plus the windage loss shall not exceed 5-watts/ft-lb-sec (of maximum wheel design value) under the worst case internal pressure and temperature; operating at maximum momentum in the counter-rotation mode in a zero-g field.

#### 3.2.4 Life

3.2.4.1 Storage and Calendar - The reaction wheel shall be designed to have a minimum life, whether operating or not, of 100,000 hours when subjected to all environmental requirements of this specification except shock, vibration, and ascent pressure decay.

3.2.4.2 Operating - The reaction wheel shall be designed such that after operation for 10-years a comparative set of data regarding bearing losses at a given temperature shall not deviate from an initial set by more than one-percent.

3.2.4.3 Starts, Stops - The reaction wheel shall be designed to survive 2000 start-stop cycles in a one-g environment and still meet the performance requirements of this specification. Static pressure to provide bearing lift-off during start or stop is not permitted. The middle spin element will not be required to start or stop while undergoing the vibration or shock environments of paragraph 3.3.

3.2.4.4 Drive Power Loss - The reaction wheel shall be designed such that loss of drive power to either rotating member shall not cause a catastrophic failure of the reaction wheel.

### 3.3 ENVIRONMENTAL REQUIREMENTS

3.3.1 Non-Operating Environments - The reaction wheel shall be designed to meet the performance requirements of paragraph 3.2 after exposure to the environments and range thereof set forth below.

3.3.1.1 Random Vibration - As shown in Figure 1 along three orthogonal axes one of which is parallel to the spin rotation axis.

3.3.1.2 Sinusoidal Vibration - Ten-g peak from 30 - 2000 Hz for 5-minutes along the spin rotation axis, and 5-minutes along any axis normal to the spin axis.

3.3.1.3 Shock - As shown in Figure 2. Three (3) shocks in each direction along the axes described in paragraph 3.3.1.1 for a total of eighteen (18) shocks.

3.3.1.4 Sustained Acceleration - Zero to twelve-g along any of the axes described in paragraph 3.3.1.1 in either direction.

3.3.1.5 Pressure - Zero to fifteen psia.

3.3.1.6 Temperature -  $-10^{\circ}\text{C}$  to  $+50^{\circ}\text{C}$ .

3.3.1.7 Ascent Pressure Decay - The reaction wheel case shall be designed to withstand a pressure decay rate of 1.0 to 1.4 inches of Hg per-second for a period of twenty-seconds.

3.3.1.8 Humidity - Zero to one-hundred percent relative, including condensation in the form of water or frost.

3.3.2 Operating Environments - The reaction wheel shall be designed to meet the performance requirements of paragraph 3.2 during and after exposure to the environments and range thereof set forth below.

3.3.2.1 Random Vibration - As shown in Figure 3 along the same axes as in paragraph 3.3.1.1.

3.3.2.2 Temperature -  $-30^{\circ}\text{C}$  to  $+50^{\circ}\text{C}$ .

3.3.2.3 Pressure - Zero to fifteen psia.

3.3.2.4 Humidity - As in paragraph 3.3.1.8.

3.3.2.5 Sustained Acceleration - Plus one-g along any axis and at zero-g along all axes.

4.0 QUALITY ASSURANCE AND TEST REQUIREMENTS - TBS

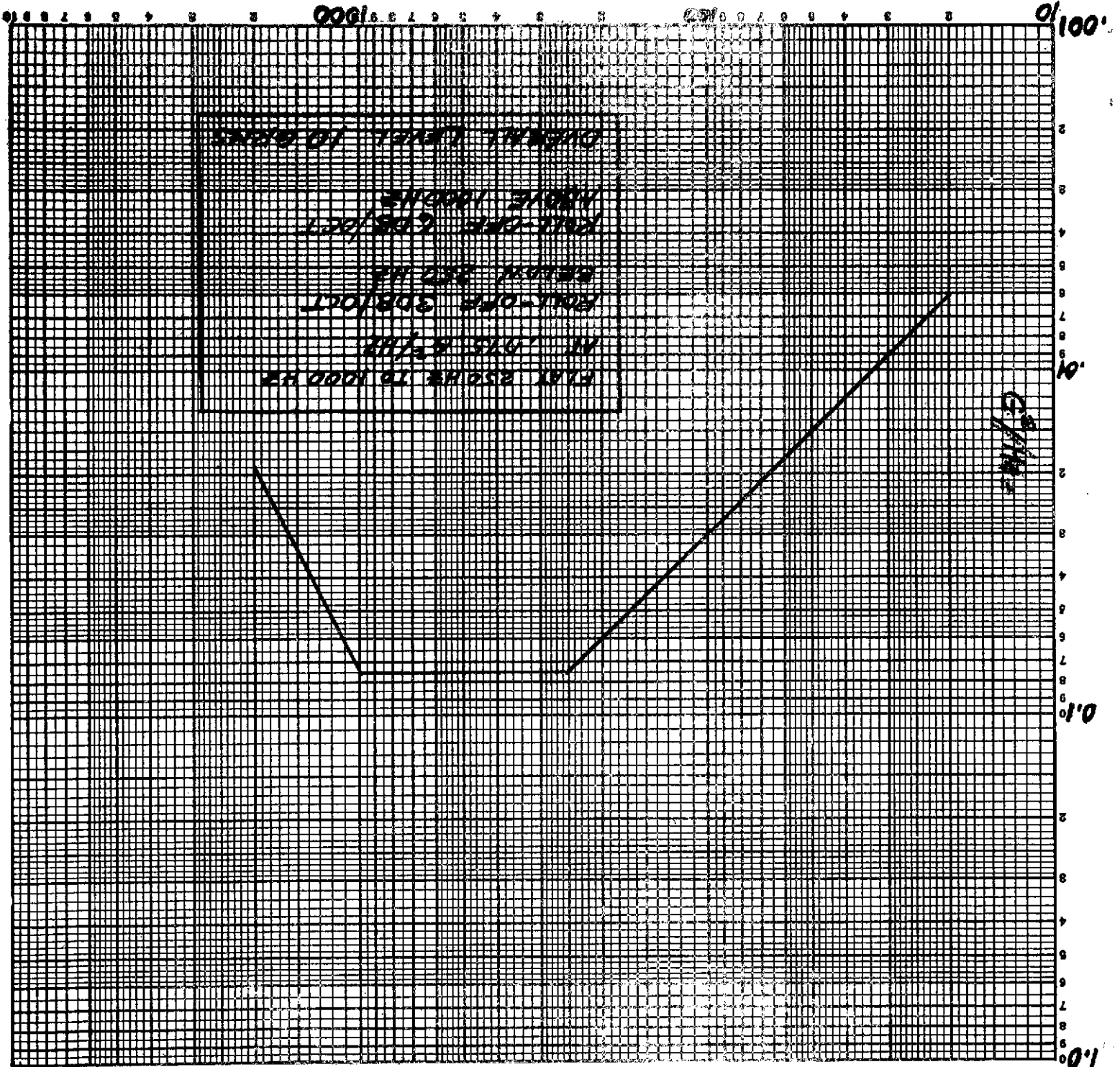
5.0 PREPARATION FOR DELIVERY - TBS

6.0 NOTES

6.1 Abbreviations - TBS: To Be Supplied.

Fig. 1

FREQUENCY - Hz



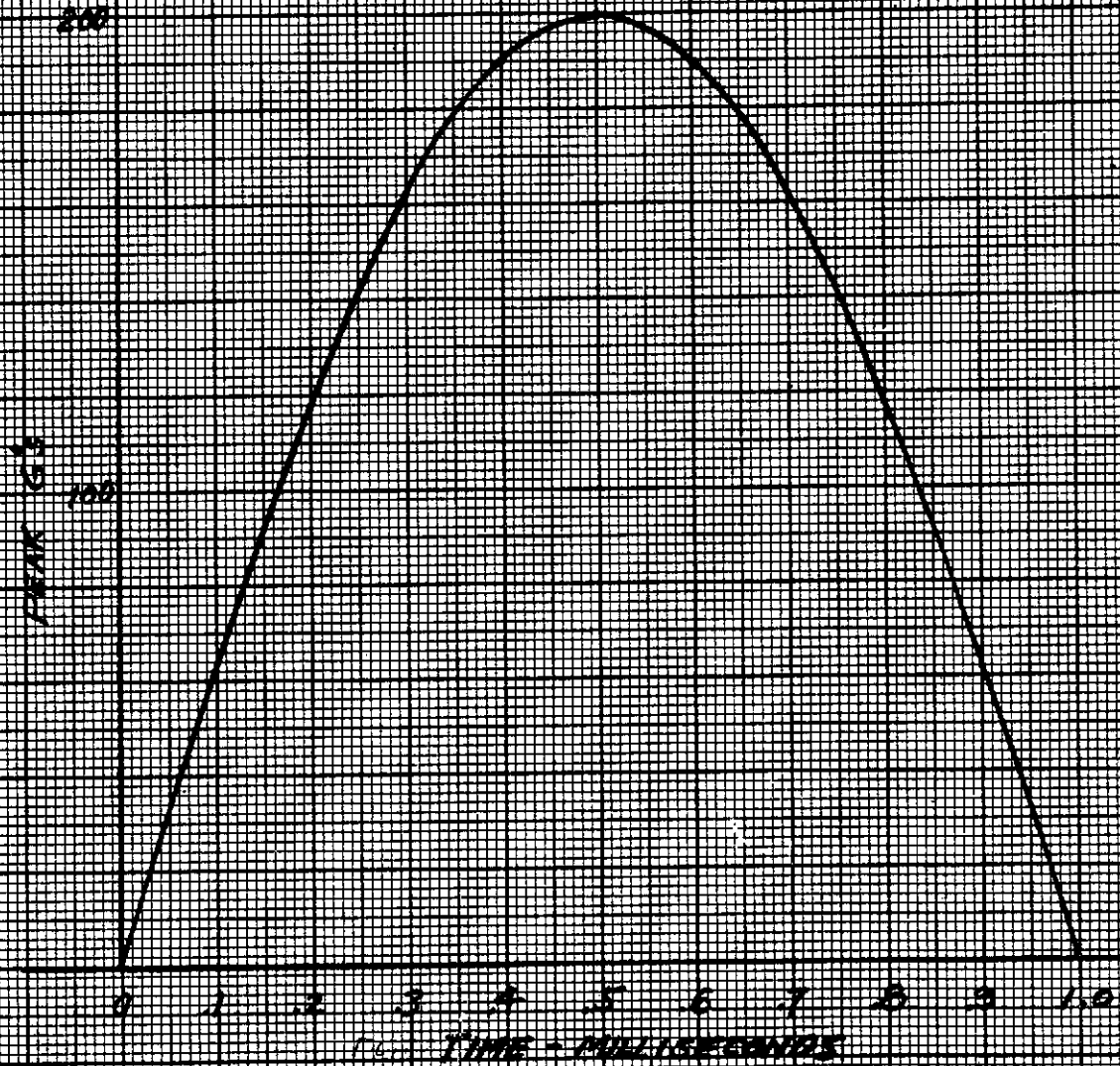
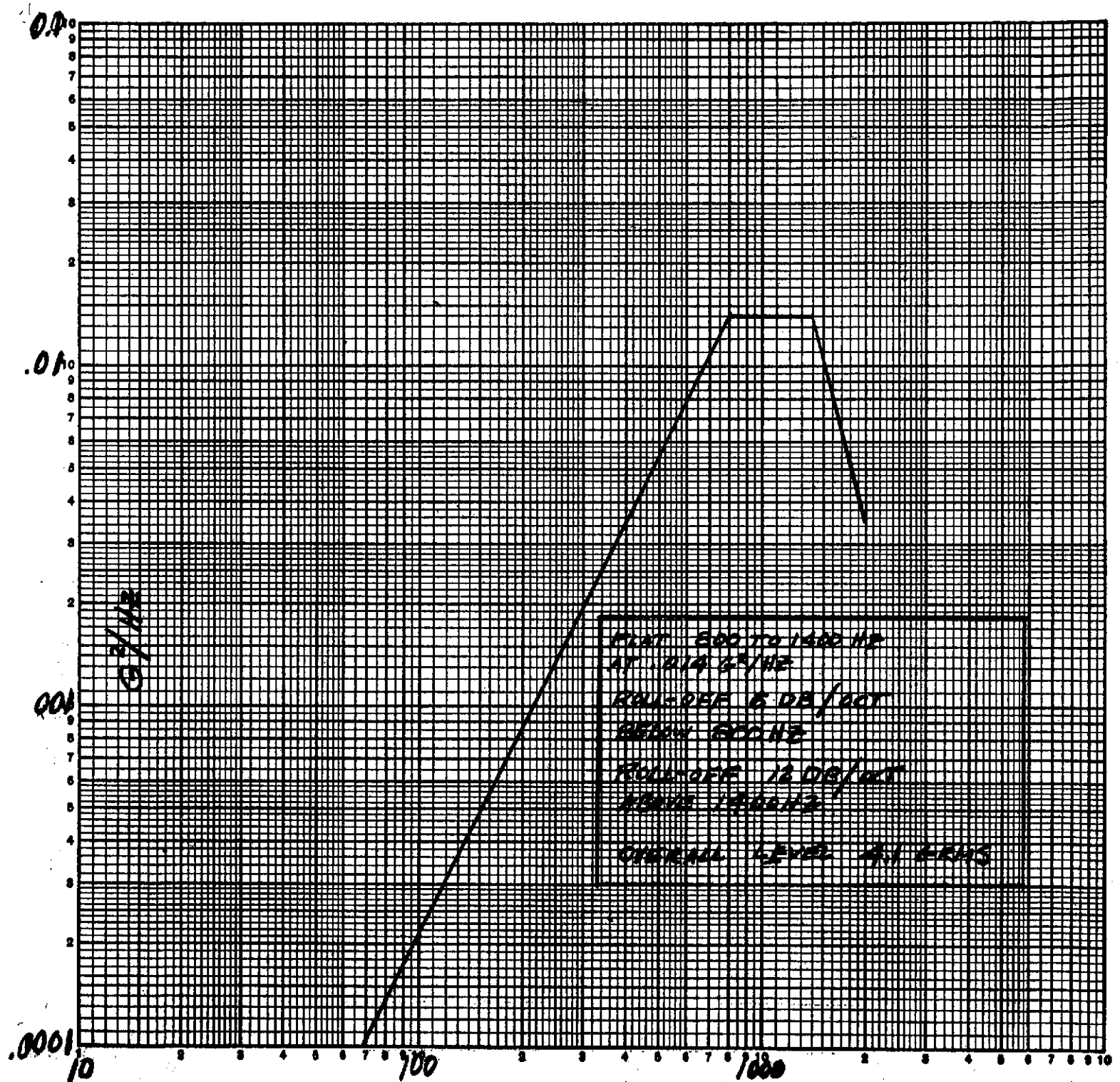


FIGURE 21



FREQUENCY - Hz

FIG. 3